

Topological phases and delocalization of quantum walks in random environments

Hideaki Obuse* and Norio Kawakami

Department of Physics, Kyoto University, Kyoto 606-8502, Japan

(Received 28 August 2011; revised manuscript received 15 November 2011; published 28 November 2011)

We investigate one-dimensional (1D) discrete-time quantum walks (QWs) with spatially or temporally random defects as a consequence of interactions with random environments. We focus on the QWs with chiral symmetry in a topological phase, and reveal that chiral symmetry together with the bipartite nature of the QWs brings about intriguing behaviors such as coexistence of topologically protected edge states at zero energy and Anderson transitions in the 1D chiral class at *nonzero* energy in their dynamics. In contrast to results of previous studies, therefore, the spatially disordered QWs can avoid complete localization due to the Anderson transition. It is further confirmed that the edge states are robust to spatial disorder but not to temporal disorder.

DOI: [10.1103/PhysRevB.84.195139](https://doi.org/10.1103/PhysRevB.84.195139)

PACS number(s): 73.20.Fz, 03.67.–a, 05.40.Fb, 03.65.Yz

I. INTRODUCTION

A quantum walk¹ (QW) describes quantum mechanical time evolution of particles, which is identified as a random walk when the system is brought to the classical limit. The QW may provide a unique avenue to realize quantum computation since the QW can be applied for efficient algorithms of quantum computation.^{2,3} Among several kinds of QWs, the two-state discrete-time QW in one dimension (1D) has been intensively investigated due to its simple formalism. More remarkably, it has been experimentally realized in various systems, such as cold atoms,⁴ trapped ions,^{5,6} and photons.^{7–9} The discrete-time QW is described by two basic operators. The coin operator C defined as

$$C \equiv \begin{pmatrix} \cos \theta & -\sin \theta \\ \sin \theta & \cos \theta \end{pmatrix} \quad (1)$$

acts on two internal states, right and left walkers $|R\rangle$ and $|L\rangle$, respectively. The shift operator S is defined as

$$S \equiv \sum_{n=-N/2}^{N/2-1} (|n+1\rangle\langle n| \otimes |R\rangle\langle R| + |n-1\rangle\langle n| \otimes |L\rangle\langle L|), \quad (2)$$

so that each walker moves from a position n to its corresponding neighbor $n \pm 1$. Here, N represents the system length. The time evolution operator U is built up from these two operators and the corresponding Hamiltonian H is defined through

$$U \equiv S \left(\sum_n |n\rangle\langle n| \otimes C \right) = e^{iH\delta t}, \quad (3)$$

where δt is a unit of time and we hereafter set $\delta t = 1$. Thus, a state at time t , $|\psi(t)\rangle$, is given by $|\psi(t)\rangle = U^t |\psi(0)\rangle$ starting from an initial state $|\psi(0)\rangle$.

It is known that the Hamiltonian H described by Eqs. (1)–(3) is equivalent to the Dirac equation in the continuum limit.^{10,11} Recently, symmetries of the Hamiltonian, which are relevant to classify topological phases,^{12,13} were examined in Ref. 14, and it was found that the QW described by Eqs. (1)–(3), which has been realized in many experiments,^{4–8} possesses chiral symmetry. Reference 14 clarified that the Dirac equation derived from the 1D QW with chiral symmetry gives a finite Berry phase and thus generates edge states near boundaries, since 1D chiral classes can be characterized

by an integer topological number.^{12,13} The edge states in the topological phase would also be useful for topological quantum computation,^{15–17} if the system is described by Majorana fermions, which is currently a subject of intensive studies in condensed matter physics.

Understanding of the effects of the interaction with environments giving rise to decoherence is a key issue in realizing quantum computation.¹⁸ To this end, there are theoretical^{19–25} and experimental^{4,7–9} studies of discrete-time QWs taking account of spatial and/or temporal disorders. It is found that Anderson localizations occur for QWs with spatial disorder while QWs with temporal disorder approach classical random walks.

In this work, we investigate two-state discrete-time 1D QWs described by Eqs. (1)–(3), which belong to the chiral orthogonal class, interacting with spatially or temporally random defects. In contrast to the previous studies, we reveal that the QWs with spatial disorder exhibit delocalized behaviors. This remarkable conclusion is drawn from extensive numerical calculations and is further ensured by symmetry arguments for the 1D chiral class. We also find that the edge states in the topological phase are robust for spatial disorder but not for temporal disorder.

This paper is organized as follows. In Sec. II, we give general remarks on QWs without any disorder and demonstrate that the edge states are induced by introducing a reflecting coin operator. Our main results for the spatially or temporally disordered QWs are presented in Sec. III. Section IV is devoted to discussions and summary.

II. QUANTUM WALKS WITH REFLECTING COIN OPERATORS

Let us first explain eigenstates of the QW. The eigenenergy ω_λ of the QW, which has periodicity of 2π , is defined through the eigenvalue of the time-evolution operator by $U|\psi_\lambda\rangle = e^{i\omega_\lambda}|\psi_\lambda\rangle$, where $|\psi_\lambda\rangle$ is the corresponding eigenstate. Hereafter, the subscript λ is written only when we need to emphasize it. The dispersion relation resulting from Eqs. (1)–(3) is given by $\cos(\omega) = \cos(k)\cos(\theta)$, where k is the wave number.^{11,14} Since the energy gap should exist to support edge states in topological phases, edge states of the QW are able to appear when $\theta \neq 0, \pi$.

To generate the edge states, a boundary should be prepared for the QW. While a split-step method is proposed in Ref. 14,

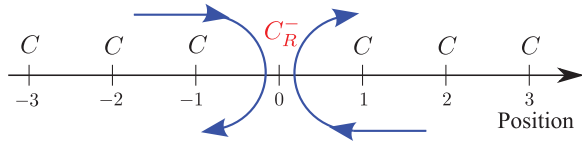


FIG. 1. (Color online) The QW with a reflecting coin operator at the origin.

we employ a simpler method to make the boundary in terms of a reflecting coin operator defined as

$$C_R^\pm \equiv \begin{pmatrix} 0 & \mp 1 \\ \pm 1 & 0 \end{pmatrix}, \quad (4)$$

so that a right walker is changed to a left walker and vice versa. Thereby, C_R^\pm realizes a hard-wall boundary. The sign of the reflecting coin operator determines the presence or absence of edge states.^{26,27} In the case of Hadamard walks ($\theta = \pi/4$), the edge states appear if C_R^- is introduced at the boundary.

We now consider the Hadamard walks with C_R^- at the origin as shown in Fig. 1. The initial state is prepared as

$$|\psi(0)\rangle \equiv |0\rangle \otimes (|R\rangle + i|L\rangle)/\sqrt{2} \quad (5)$$

throughout the paper, so that the right and left walkers do not mix with each other due to real-number elements of the coin operator, and thus the probability distribution becomes symmetric in the absence of spatial disorder. Figure 2(a) shows the probability distribution $P_n(t)$ at $t = 80$, which is defined as

$$P_n(t) \equiv \sum_{\sigma=R,L} | \langle n | \otimes \langle \sigma | \psi(t) \rangle |^2. \quad (6)$$

We find a sharp peak at the origin due to edge states in the topological phase and two smaller peaks near $n \sim \pm 50$ commonly observed in QWs.^{2,3} Note that these observations

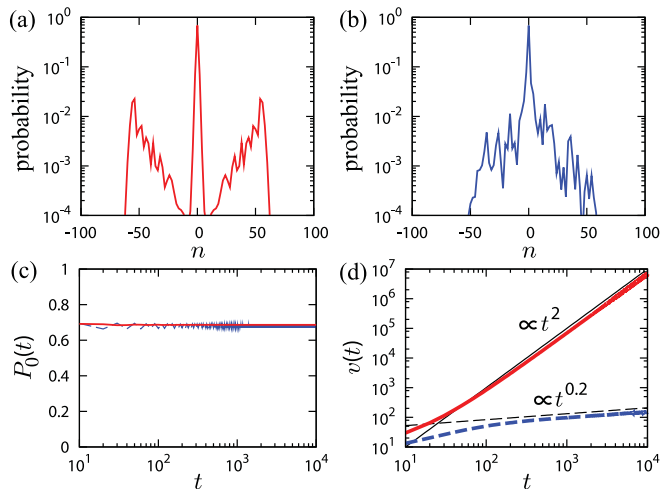


FIG. 2. (Color online) Probability distributions at $t = 80$ of the QWs with $\delta\theta_s = 0$ (a) and $\pi/4$ (b) with C_R^- for a single sample. t dependence of the survival probability $P_0(t)$ (c) and the variance $v(t)$ (d). In (c) and (d), the solid and dashed curves represent the QWs with $\delta\theta_s = 0$ and $\pi/4$, respectively. The two thin lines in (d) indicate power law behaviors. The number of samples is 10^4 in the case of disordered QWs.

are consistent with the recently derived limit measure²⁷ at $t \rightarrow \infty$ for the 1D QW on a half line. The time dependence of the survival probability

$$P_0(t) \equiv P_n(t)|_{n=0} \quad (7)$$

and the position variance of the QWs

$$v(t) \equiv \langle \psi(t) | n^2 | \psi(t) \rangle - [\langle \psi(t) | n | \psi(t) \rangle]^2 \quad (8)$$

are shown by solid curves in Figs. 2(c) and 2(d), respectively. We confirm that the edge states are robust to time evolution since $P_0(t)$ keeps its value unchanged and $v(t)$ is proportional to t^2 , which agrees with results for ordinary QWs.^{2,3}

III. DISORDERED QUANTUM WALKS

Next, we consider disordered QWs. We assume that disorder is introduced via fluctuations of θ in Eq. (1), which do not break chiral symmetry. To this end, we redefine θ so that θ is randomly distributed over positions n or time t as

$$\theta \in [\bar{\theta} - \delta\theta_{s(t)}/2 : \bar{\theta} + \delta\theta_{s(t)}/2],$$

where $\bar{\theta}$ represents the mean value of distributed θ and $\delta\theta_{s(t)}$ indicates the strength of spatial (temporal) disorder. We hereafter restrict our attention to QWs with $\bar{\theta} = \pi/4$ and with either spatial or temporal disorder.

A. Spatially disordered quantum walks

Let us begin with the spatial disorder. The probability distribution $P_n(t)$ for spatially disordered QWs with C_R^- after 80 time steps is shown in Fig. 2(b). The peak at the origin due to the edge states seems to be robust for the spatial disorder. The survival probability $P_0(t)$ indeed ensures this point: the profile of $P_0(t)$ is almost unchanged from that for the clean QW. On the other hand, the outer two smaller peaks existing in Fig. 2(a) disappear in Fig. 2(b), implying that the QWs suffer from the spatial disorder except for their edge states. In this case, the Anderson localization would be important as studied in previous work.^{9,20,21} If the Anderson localization completely dominates the dynamics of QWs, the variance $v(t)$ should become a constant after many time steps. However, $v(t)$ for the spatially disordered QWs [Fig. 2(d)] exhibits a power law behavior with a smaller exponent, suggesting that the QWs show anomalous diffusion even in the presence of spatial disorder.

To address the above point, we look into the density of states (DOS) $\rho(\omega)$, which provides us with a clear-cut interpretation of the seemingly peculiar dynamics of the QWs. Note that a state $|\psi(t)\rangle$ is considered as the superposition of all the eigenstates because we employ a δ -function-like initial state $|\psi(0)\rangle$. The DOS for a clean QW with translational symmetry is given by

$$\rho_c(\omega) = \frac{\sin \omega}{2\pi \sqrt{\cos^2 \theta - \cos^2 \omega}} \quad \text{for } \cos^2 \omega < \cos^2 \theta. \quad (9)$$

When $\cos^2 \omega = \cos^2 \theta$ at $\theta \neq 0, \pi$, $\rho_c(\omega)$ diverges due to the Van Hove singularity. For the QW with C_R^- , we find that the DOS consists of $\rho_c(\omega)$ and doubly degenerate states at $\omega = 0, \pi$ as shown in Fig. 3(a). According to the nature of $|\psi_\lambda\rangle$ for $\omega_\lambda = 0, \pi$, these states are identified as the edge states in the

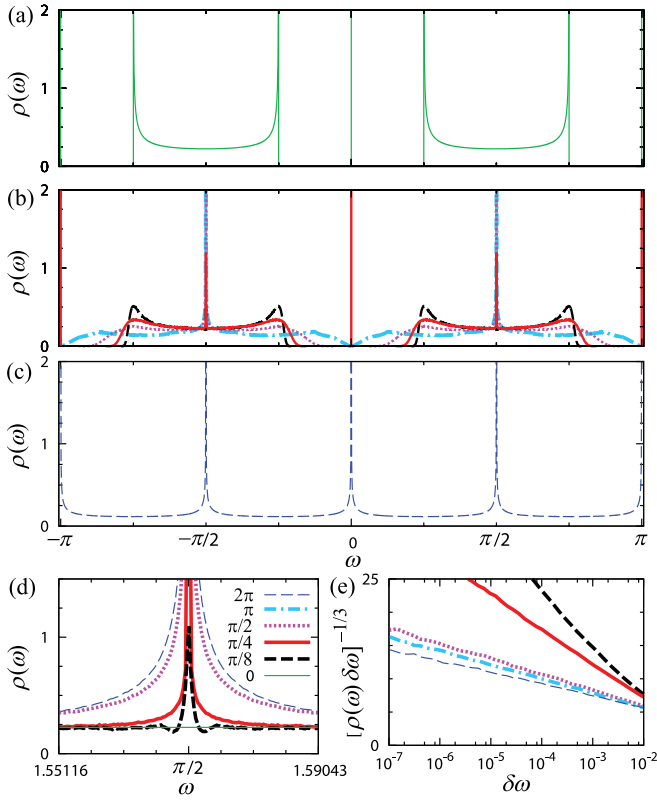


FIG. 3. (Color online) DOS $\rho(\omega)$ for QWs with C_R^- for $\delta\theta_s = 0$ (a), $\delta\theta_s = \pi/8, \pi/4, \pi/2$, and π (b), and 2π (c). $N = 500$ and the number of samples is 10^5 for each $\delta\theta_s$ ($\neq 0$). (d) The enlargement of the DOS around $\omega = \pi/2$ for QWs with various $\delta\theta_s$. (e) The scaling collapses into Eq. (10) for the DOS near $\omega = \pi/2$ for QWs of the larger system $N = 10^4$ with 10^4 samples. The labels in (d) represent values of $\delta\theta_s$. In calculations of the DOS, periodic boundary conditions are imposed on both edges of the 1D QW.

topological phase. In the clean QW, therefore, the edge states appear not only at $\omega = 0$ but also at $\omega = \pi$. With increasing $\delta\theta_s$ [Fig. 3(b)], the divergences in the DOS at $\omega = \pm\pi/4$ and $\pm 3\pi/4$ are rounded since the Van Hove singularity is not well defined for disordered systems. Furthermore, we notice that the energy gaps around $\omega = 0, \pi$ are reduced while the δ functions due to edge states robustly remain.

Remarkably, there appear additional divergences in the DOS at $\omega = \pm\pi/2$ for spatially disordered QWs [Fig. 3(b)]. We give attention to the divergences in $\rho(\omega)$ at $\omega = \pm\pi/2$ by showing an enlarged picture of the DOS near $\omega = \pi/2$ in Fig. 3(d). We find that the divergence becomes stronger with increasing $\delta\theta_s$ and the DOS for the smallest disorder ($\delta\theta_s = \pi/8$) shows oscillating behavior. This oscillation reminds us of the DOS derived from chiral random matrix theories.²⁸ Indeed, a system belonging to the 1D chiral class is known to show an Anderson transition at *zero energy*, which is accompanied by a divergence in the DOS.²⁹ Although the energy at which the DOS diverges is different from what we observed for the QW, we claim that *an Anderson transition in the 1D chiral class occurs in a spatially disordered QW at $\omega = \pm\pi/2$* . This is supported by the following symmetry arguments. Chiral symmetry gives the constraint that eigenenergies appear in pairs of opposite sign, and this makes the zero-energy states in

chiral classes singular. In QWs, chiral symmetry leads to the eigenvalues of U appearing in pairs as $e^{\pm i\omega_\lambda}$. In addition, since S in Eq. (2) gives only nearest-neighbor hopping, U in Eq. (3) has a bipartite structure and the eigenvalues of U also appear in pairs as $\pm e^{i\omega_\lambda}$.³⁰ Thereby, there are four eigenenergies related to each other,

$$(\omega_\lambda, -\omega_\lambda, \omega_\lambda + \pi, -\omega_\lambda + \pi).$$

Redefining ω_λ as $\omega_\lambda = \omega'_\lambda + \pi/2$, we rewrite these eigenenergies as

$$(\omega'_\lambda + \pi/2, -\omega'_\lambda - \pi/2, \omega'_\lambda + 3\pi/2, -\omega'_\lambda + \pi/2).$$

One finds that the first and fourth (second and third) eigenenergies appear in pairs with respect to $\omega = \pi/2$ ($-\pi/2$),³¹ making $\omega = \pm\pi/2$ special energies as in the zero energy of ordinary chiral classes. We therefore come to the conclusion that the Anderson transition of the 1D chiral class should occur at $\omega = \pm\pi/2$ even if there are energy gaps and the edge states exist at $\omega = 0, \pi$.

According to universality, the same critical behaviors near zero energy studied with a tight-binding Hamiltonian in Ref. 29 should be observed in the discrete-time QW near $\omega = \pm\pi/2$. Thereby, we write down the modified formulas for divergences of the DOS ρ and the localization length ξ , defined as the inverse of Lyapunov exponents, at $\omega = \pm\pi/2$ as

$$\rho(\omega) = \rho_0 [\delta\omega\tau |\ln^3(\delta\omega\tau)|]^{-1}, \quad (10)$$

$$\xi(\omega) = \xi_0 |\ln(\delta\omega\tau)|, \quad (11)$$

respectively, where $\delta\omega \equiv |\omega \mp \pi/2|$ represents the distance from the critical points $\omega = \pm\pi/2$. τ denotes the mean free time and ρ_0 and ξ_0 are constants. As shown in Fig. 3(e), we verify that the DOS near $\omega = \pi/2$ obeys Eq. (10) fairly well.

We also calculate the localization length ξ of the spatially disordered QW near $\omega = \pi/2$ by using the transfer matrix method.^{20,32} By rearranging the wave function amplitudes around the position n of the eigenvalue equation $U|\psi\rangle = e^{i\omega}|\psi\rangle$, we obtain the iterative relation

$$\begin{pmatrix} \psi_{n+1,R} \\ \psi_{n,L} \end{pmatrix} = T_n \begin{pmatrix} \psi_{n,R} \\ \psi_{n-1,L} \end{pmatrix}, \quad (12)$$

$$T_n = \begin{pmatrix} e^{-i\omega}/\cos\theta_n & -\tan\theta_n \\ -\tan\theta_n & e^{i\omega}/\cos\theta_n \end{pmatrix}, \quad (13)$$

where $\psi_{n,\sigma=R,L}$ represents the wave function amplitude of the right or left walker at the position n and θ_n denotes θ at the position n . The huge system length $N = 10^8$ allows us to evaluate accurate numerical values of ξ .

Figure 4(a) shows the $\delta\omega$ dependence of ξ for various $\delta\theta_s$. We confirm that ξ for any $\delta\theta_s$ shows the diverging behavior in the vicinity of $\delta\omega = 0$ while ξ for $\delta\omega \neq 0$ is finite, resulting in Anderson localization. Although the numerical restriction of $\delta\omega \gtrsim 10^{-16}$ prevents us from reaching $\xi \rightarrow \infty$ with accuracy, we confirm that ξ follows Eq. (11) as shown in Fig. 4(b). This scaling collapse gives evidence that ξ diverges at $\delta\omega = 0$ for any $\delta\theta_s$. In this case, the transport property is anomalous because it involves algebraic decays instead of exponential ones.³⁴ Hence, the walkers can move around through these delocalized states at $\omega = \pm\pi/2$ and then $v(t)$ indicates anomalous diffusion as shown in

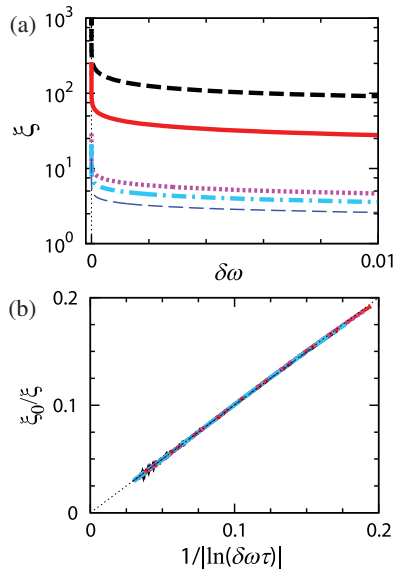


FIG. 4. (Color online) (a) Dependence on $\delta\omega$ of the localization length ξ of the QWs with $\delta\theta_s = \pi/8, \pi/4, \pi/2, \pi,$ and 2π from the top to the bottom. (b) The scaling collapse into Eq. (11) for ξ in (a). The parameters ξ_0 and τ are obtained by fitting. The dotted thin line represents Eq. (11).

Fig. 2(d). Interestingly, three kinds of state (edge, localized, and delocalized states) simultaneously appear in dynamics of spatially disordered QWs with C_R^- . This coexistence occurs not only for the specific initial state, Eq. (5), but also for general δ -function-like initial states, so that the dynamics of QWs is described by all the eigenstates. We mention that, since the coin operator of previous work^{9,19–21} for 1D spatially disordered QWs does not retain chiral symmetry, the Anderson transition is not found and only the Anderson localized states are confirmed.

It is known for zero-energy states of chiral classes³³ and various topological insulators, such as the integer quantum Hall transition, that topologically protected edge states stably exist unless the bulk band gap is closed. When a symmetry-preserving perturbation collapses the bulk gap, the delocalized states which can be coupled with the edge states so that the topological number is changed should appear even in 1D disordered systems. In other words, the existence of delocalized states due to the Anderson delocalization is essential to topological phases in disordered systems. It is naturally expected, then, that the 1D QW with chiral symmetry also follows a similar fashion under spatial disorder of θ .

Here, we clarify how the strong spatial disorder $\delta\theta_s$ induces delocalized states at $\omega = 0, \pi$ as a consequence of the gap closing. Figure 3(b) indicates that the bulk gaps around $\omega = 0, \pi$ become smaller with increasing $\delta\theta_s$, although there still remain the edge states at $\delta\theta_s = \pi$. Unfortunately, it is difficult to find the gap closing from the DOS since the finite system calculation keeps the mean level spacing finite. Alternatively, we calculate the localization length ξ at $\omega = 0$ for the QW without C_R^- for various $\delta\theta_s$ by using Eqs. (12) and (13). Note that when the bulk gap around $\omega = 0$ is finite, the localization length is interpreted as that of an exponentially decaying evanescent mode. Figure 5 clearly shows that the

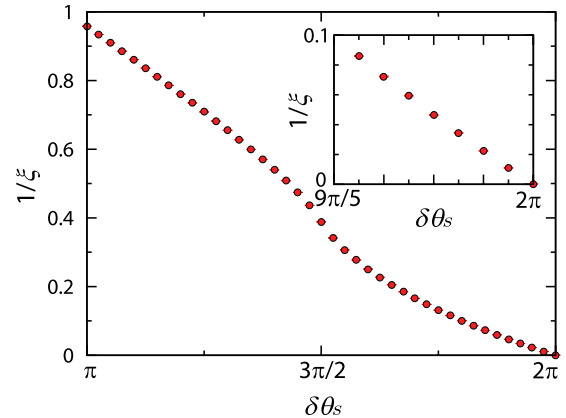


FIG. 5. (Color online) $\delta\theta_s$ dependence of the inverse of the localization length at $\omega = 0$. The length of the system is $N = 10^8$. Inset: Enlargement of ξ^{-1} near $\delta\theta_s = 2\pi$.

localization length ξ at $\omega = 0$ increases with increasing $\delta\theta_s$, and finally diverges at $\delta\theta_s = 2\pi$, where θ is fully distributed in 2π rad. This suggests that the bulk gap around $\omega = 0$ is closed. Figure 3(c) shows the DOS $\rho(\omega)$ at $\delta\theta_s = 2\pi$. We confirm that, instead of the δ functions of the edge states, divergences in the DOS, which are the same as those at $\omega = \pm\pi/2$, appear even at $\omega = 0, \pi$. Therefore, Anderson transitions occur at $\omega = 0, \pi$ as well as $\pm\pi/2$ at $\delta\theta_s = 2\pi$, and the coexistence of edge and delocalized states does not occur.

B. Temporally disordered quantum walks

Finally, we consider QWs with temporal disorder where θ in Eq. (1) is shuffled in each time step. It is known that, since the temporal disorder gives rise to decoherence, the QWs approach the classical random walks where the probability distribution of QWs becomes Gaussian and the

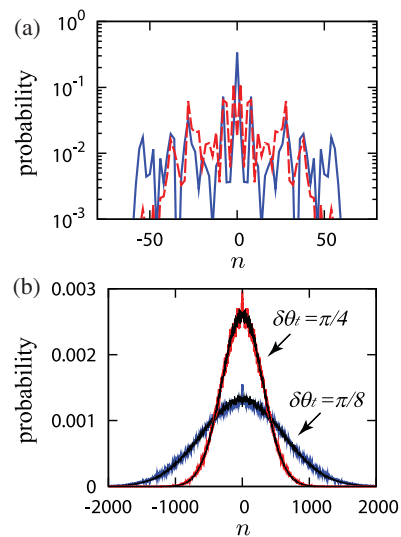


FIG. 6. (Color online) Probability distributions at $t = 80$ for a single sample (a) and sample-averaged probability distributions at $t = 10^4$ (b) of temporally disordered QWs. The solid and dashed curves represent QWs with $\delta\theta_t = \pi/8$ and $\pi/4$, respectively, and the thick and thin curves distinguish QWs with and without C_R^- , respectively. The number of samples is 10^4 .

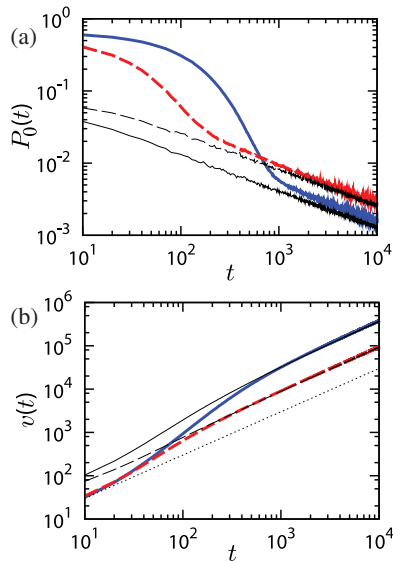


FIG. 7. (Color online) t dependence of the survival probability $P_0(t)$ (a) and the variances $v(t)$ (b). The solid and dashed curves represent QWs with $\delta\theta_t = \pi/8$ and $\pi/4$, respectively, and the thick and thin curves distinguish QWs with and without C_R^- , respectively. The number of samples is 10^4 . The dotted line in (b) indicates $v(t) \propto t$.

position variance $v(t)$ is proportional to t .^{22–25} We study how the edge states of the QWs with C_R^- are affected by the temporal disorder. The probability distribution $P_n(t)$ after 80 time steps in Fig. 6(a) demonstrates that the peaks due to the edge states are substantially reduced with increasing $\delta\theta_t$. For longer time steps $t = 10^4$, the sample-averaged $P_n(t)$ with temporal disorder [Fig. 6(b)] become Gaussian, indicating that the QWs approach classical random walks. Tiny peaks at the origin, which are the remnants of the edge states, are found for the QWs with C_R^- . In Fig. 7(a), the survival probabilities $P_0(t)$ of QWs with C_R^- are compared with those without C_R^- . We find that $P_0(t)$ of the former QWs behaves differently from that of the latter during rather short time steps, while at longer time steps they converge to the same curve, which means that the edge states gradually disappear. The position variance $v(t)$ in Fig. 7(b) increases linearly in time for longer time steps, clarifying that the QWs with edge states are also transformed into classical random walks.

IV. DISCUSSION AND SUMMARY

In this work, we have focused only on discrete-time QWs. Here some comments are in order on the relevance of our results to continuous-time QWs with spatial disorder. While the 1D continuous-time QW with on-site random potentials has been studied previously,^{35,36} the corresponding Hamiltonian

does not retain chiral symmetry. We note that the Hamiltonian of the 1D continuous-time QW possessing chiral symmetry is the tight-binding model with only nearest-neighbor random hopping terms. Indeed, the latter model is consistent with the one studied in Ref. 29, and the Anderson transition is possible only at zero energy, in contrast to the discrete-time QWs studied in the present work. Therefore, the coexistence of edge states and the Anderson transition is peculiar to discrete-time QWs.

We also mention that, although we have been concerned with QWs with C_R^- here, our conclusion can be directly applied for QWs without C_R^- , except for the argument on edge states at $\omega = 0, \pi$.

In summary, we have investigated two-state discrete-time QWs belonging to the 1D chiral orthogonal class in the presence of spatial or temporal disorder. We have elucidated that Anderson transitions in the 1D chiral classes occur at $\omega = \pm\pi/2$ in QWs with any strength of spatial disorder and thereby the QWs can avoid complete localization. We note that, while the currently available experiments on discrete-time QWs can accomplish only a few tens of time steps and it may be difficult to completely eliminate the temporal disorder giving rise to decoherence in spatially disordered QWs, the delocalization behavior found in the present work will be observed when the technology of QWs is further developed in the applications of quantum computers.

Furthermore, we have shown that the coexistence of edge, localized, and delocalized states is realized in the time evolution of a spatially disordered QW with C_R^- . This characteristic nature of the QWs is supported by chiral symmetry of H and bipartite structures of U . We predict that delocalization of QWs with spatial disorder should be observed in a wide variety of 1D QWs belonging to other chiral classes¹⁴ and to classes D and DIII which are described by Majorana fermions, since these universality classes also show the Anderson transition in 1D.^{37,38} QWs for which tuning of the system parameters and observation of walkers' probabilities are possible in experiments would provide an intriguing arena in which to study topological phases for systems with defects and decoherence.

Note added. We recently became aware of Ref. 39 in which the edge states of QWs are observed in experiments.

ACKNOWLEDGMENTS

We acknowledge fruitful discussions with T. Oka. H.O. is supported by a Grant-in-Aid from JSPS for Young Scientists, and N.K. by KAKENHI (Grants No. 21740232 and No. 20104010) and JSPS through the ‘‘Funding Program for World-Leading Innovative R&D on Science and Technology’’ (FIRST Program).

*Present address: Institut für Nanotechnologie, Karlsruhe Institute of Technology, 76021 Karlsruhe, Germany.

¹Y. Aharonov, L. Davidovich, and N. Zagury, *Phys. Rev. A* **48**, 1687 (1993).

²J. Kempe, *Contemp. Phys.* **44**, 307 (2003).

³A. Ambainis, *Int. J. Quantum Inform.* **1**, 507 (2003).

⁴M. Karski, L. Förster, J.-M. Choi, A. Steffen, W. Alt, D. Meschede, and A. Widera, *Science* **325**, 174 (2009)

- ⁵H. Schmitz, R. Matjeschk, Ch. Schneider, J. Glueckert, M. Enderlein, T. Huber, and T. Schaetz, *Phys. Rev. Lett.* **103**, 090504 (2009).
- ⁶F. Zähringer, G. Kirchmair, R. Gerritsma, E. Solano, R. Blatt, and C. F. Roos, *Phys. Rev. Lett.* **104**, 100503 (2010).
- ⁷A. Schreiber, K. N. Cassemiro, V. Potoček, A. Gábris, P. J. Mosley, E. Andersson, I. Jex, and Ch. Silberhorn, *Phys. Rev. Lett.* **104**, 050502 (2010).
- ⁸M. A. Broome, A. Fedrizzi, B. P. Lanyon, I. Kassal, A. Aspuru-Guzik, and A. G. White, *Phys. Rev. Lett.* **104**, 153602 (2010).
- ⁹A. Schreiber, K. N. Cassemiro, V. Potoček, A. Gábris, I. Jex, and Ch. Silberhorn, *Phys. Rev. Lett.* **106**, 180403 (2011).
- ¹⁰D. A. Meyer, *J. Stat. Phys.* **85**, 551 (1996).
- ¹¹F. W. Strauch, *Phys. Rev. A* **73**, 054302 (2006).
- ¹²A. P. Schnyder, S. Ryu, A. Furusaki, and A. W. W. Ludwig, *Phys. Rev. B* **78**, 195125 (2008).
- ¹³A. Kitaev, in *Advances in Theoretical Physics*, edited by V. Lebedev and M. Feigel'man, AIP Conf. Proc. No. 1134 (AIP, Melville, NY, 2009), p. 22.
- ¹⁴T. Kitagawa, M. S. Rudner, E. Berg, and E. Demler, *Phys. Rev. A* **82**, 033429 (2010).
- ¹⁵A. Y. Kitaev, *Phys. Usp.* **44**, 131 (2001).
- ¹⁶J. Alicea, Y. Oreg, G. Refael, F. V. Oppen, and M. P. A. Fisher, *Nat. Phys.* **13**, 1 (2011).
- ¹⁷L. Lehman, V. Zatloukal, G. K. Brennen, J. K. Pachos, and Z. Wang, *Phys. Rev. Lett.* **106**, 230404 (2011).
- ¹⁸V. Kendon, *Math. Struct. Comput. Sci.* **17**, 1168 (2007).
- ¹⁹N. Konno, *Quantum Inf. Proc.* **8**, 387 (2009).
- ²⁰A. Joye and M. Merkli, *J. Stat. Phys.* **140**, 1025 (2010).
- ²¹A. Ahlbrecht, V. B. Scholz, and A. H. Werner, *J. Math. Phys.* **52**, 102201 (2011).
- ²²T. D. Mackay, S. D. Bartlett, L. T. Stephenson, and B. C. Sanders, *J. Phys. A* **35**, 2745 (2002).
- ²³T. A. Brun, H. A. Carteret, and A. Ambainis, *Phys. Rev. Lett.* **91**, 130602 (2003); *Phys. Rev. A* **67**, 032304 (2003).
- ²⁴J. Kosik, V. Buzek, and M. Hillery, *Phys. Rev. A* **74**, 022310 (2006).
- ²⁵G. Abal, R. Donangelo, F. Severo, and R. Siri, *Physica A* **387**, 335 (2008).
- ²⁶T. Oka, N. Konno, R. Arita, and H. Aoki, *Phys. Rev. Lett.* **94**, 100602 (2005).
- ²⁷K. Chisaki, N. Konno, and E. Segawa, e-print [arXiv:1009.1306](https://arxiv.org/abs/1009.1306).
- ²⁸T. Nagao and K. Slevin, *J. Math. Phys.* **34**, 2317 (1993); J. Verbaarschot, *Nucl. Phys. B* **426**, 559 (1994).
- ²⁹F. J. Dyson, *Phys. Rev.* **92**, 1331 (1953); G. Theodorou and M. H. Cohen, *Phys. Rev. B* **13**, 4597 (1976); T. P. Eggarter and R. Riedinger, *ibid.* **18**, 569 (1978).
- ³⁰The pair of eigenvalues $\pm e^{i\omega_\lambda}$ also guarantee the edge states at $\omega_\lambda = \pi$ as counterparts of the eigenstates at $\omega_\lambda = 0$.
- ³¹Y. Shikano and H. Katsura, *Phys. Rev. E* **82**, 031122 (2010).
- ³²A. MacKinnon and B. Kramer, *Z. Phys. B* **53**, 1 (1983).
- ³³S. Ryu and Y. Hatsugai, *Phys. Rev. Lett.* **89**, 077002 (2002).
- ³⁴C. Mudry, P. W. Brouwer, and A. Furusaki, *Phys. Rev. B* **59**, 13221 (1999).
- ³⁵J. P. Keating, N. Linden, J. C. F. Matthews, and A. Winter, *Phys. Rev. A* **76**, 012315 (2007).
- ³⁶Y. Yin, D. E. Katsanos, and S. N. Evangelou, *Phys. Rev. A* **77**, 022302 (2008).
- ³⁷P. W. Brouwer, A. Furusaki, I. A. Gruzberg, and C. Mudry, *Phys. Rev. Lett.* **85**, 1064 (2000).
- ³⁸M. Titov, P. W. Brouwer, A. Furusaki, and C. Mudry, *Phys. Rev. B* **63**, 235318 (2001).
- ³⁹T. Kitagawa, M. A. Broome, A. Fedrizzi, M. S. Rudner, E. Berg, I. Kassal, A. Aspuru-Guzik, E. Demler, and A. G. White, e-print [arXiv:1105.5334](https://arxiv.org/abs/1105.5334).